Puckering Transition of 4-Substituted Proline Residues

Il Keun Song and Young Kee Kang*

Department of Chemistry and Basic Science Research Institute, Chungbuk National University, Cheongju, Chungbuk 361-763, Korea

Received: December 12, 2004; In Final Form: April 25, 2005

The puckering transition of 4-substituted proline residues by electron-withdrawing groups, i.e., 4(*R*)-hydroxy-L-proline (Hyp) and 4(*R*)-fluoro-L-proline (Flp) residues, with trans and cis prolyl peptide bonds was studied by adiabatic optimizations along the torsion angle χ^1 of the prolyl ring at the HF/6-31+G(d) level. By analyzing the potential energy surface and local minima, it is observed that the puckering transition of the prolyl ring for Hyp and Flp residues proceeds from a down-puckered conformation to an up-puckered one through the transition state with an envelope form having the N atom at the top of envelope and not a planar one for both trans and cis conformers, which is the same as found for the unsubstituted proline residue. At HF/6-31+G(d) and B3LYP/6-311++G(d,p) levels, the structures of the backbone and prolyl ring for local minima of Ac-Hyp-NHMe and Ac-Flp-NHMe are quite similar to those of Ac-Pro-NHMe. However, the relative stability of the up-puckered conformation to the down-puckered one is increased for Ac-Hyp-NHMe with the cis imide bond and for Ac-Flp-NHMe with the trans and cis imide bonds. In particular, the 4(*R*)-substitution by hydroxy and fluorine groups has brought some structural changes in the prolyl ring of the transition states and the changes in barriers for the puckering transition. The puckering transitions for Ac-Hyp-NHMe and Ac-Flp-NHMe are proven to be predominantly electronically driven by analyzing the electronic and enthalpic contributions to the barriers, as seen for Ac-Pro-NHMe.

Introduction

The proline (Pro) residue is unique in that its side chain is covalently bonded to the nitrogen atom of the peptide backbone. This leads the backbone to not form a hydrogen bond and the N−C$^\alpha$ rotation (ϕ) to be restrained to about −60°. Because of these conformational restrictions, Pro occurs in turns, in nonrepetitive structure, and at the ends of strands and helices of proteins.[1] In particular, the pyrrolidine of Pro residue is a five-membered ring that may adopt two distinct down-puckered (or C$^\gamma$-endo) and up-puckered (or C$^\gamma$-exo) conformations,[2] which have been known to be almost equally probable from analysis of X-ray structures of peptides[3−5] and proteins.[6−8] The down- and up-puckered conformations are defined as those where the C$^\gamma$ atom and the C═O group of Pro residue lie on the same and opposite sides, respectively, of the plane defined by three atoms C$^\delta$, N, and C$^\alpha$ (Figure 1).

^{13}C NMR relaxation measurements have provided abundant evidence for the interconversion between two puckerings in peptides in solution and in the solid state, whose relaxation time was estimated to be about 1−30 ps[9−11] and the apparent barrier was estimated to be about 1.3 kcal/mol for DL-proline in the solid state.[10] Although considerable empirical and quantum mechanical calculations have been carried out on various model compounds of proline residue, only a few works have focused on the transition of prolyl puckering. From empirical force field calculations on *N*-acetylproline methyl ester (Ac-Pro-OMe),[4] the conversion of ring puckering was found to proceed through a flat saddle with a barrier of 3.6 kcal/mol and a planar transition state with a barrier of 2.0 kcal/mol above the global minima, respectively. From B3LYP/6-31G(d) calculations, it was reported that the barrier to puckering transition from the up-puckered conformation to the down-puckered one is 2.1 kcal/mol for *N*-formyl-*trans*-proline amide (For-Pro-NH$_2$).[12] The barrier to puckering transition from the down-puckered conformation to the up-puckered one was estimated to be 2.7 and 3.3 kcal/mol for trans and cis conformers of *N*-acetylproline amide (Ac-Pro-NH$_2$) at the HF/6-31G(d) level, respectively.[13]

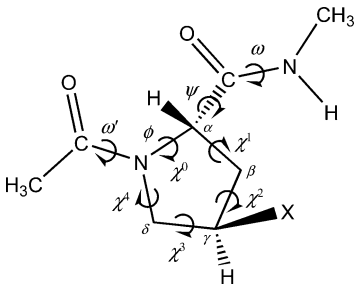

Figure 1. Definition of torsion angles and structural parameters for 4(*R*)-substituted proline dipeptides: X = OH for Ac-Hyp-NHMe; X = F for Ac-Flp-NHMe. The torsion angle χ^1 is defined for the N−C$^\alpha$−C$^\beta$−C$^\gamma$ sequence.

Recently we calculated that the puckering transition of the prolyl ring for *N*-acetyl-L-proline-*N*′-methylamide (Ac-Pro-NHMe) proceeds from a down-puckered conformation to an up-puckered one through the transition state with an envelope form having the N atom at the top of the envelope and not a planar one for both trans and cis conformers.[14] At the B3LYP/6-311++G(d,p) level, the barriers to the puckering transition $\Delta G^{\ddagger}_{\text{down}\rightarrow\text{up}}$ are estimated to be 2.58 and 3.00 kcal/mol for trans and cis conformers at room temperature, respectively. By analyzing the potential energy surface and local minima of *N*-acetyl-L-proline-*N*′,*N*′-dimethylamide (Ac-Pro-NMe$_2$) with trans and cis peptide bonds as models for polyproline II (PPII)

* Corresponding author. Telephone: +82-43-261-2285. Fax: +82-43-273-8328. E-mail: ykkang@chungbuk.ac.kr.

10.1021/jp044337p CCC: $30.25
Published on Web 08/16/2005

TABLE 1: Comparison of Barriers to Prolyl Puckering Transition

molecule	peptide bond[a]	barriers[b] (kcal/mol) down → up	barriers[b] (kcal/mol) up → down	method	ref
Ac-Pro-OMe		3.6[c,d]		empirical calculations	4
DL-proline		∼1.3[c]		^{13}C NMR relaxation	10
For-Pro-NH_2			2.1[d]	B3LYP/6-31G(d)	12
Ac-Pro-NH_2	trans	2.7[d]		HF/6-31G(d)	13
	cis	3.3[d]			
Ac-Pro-NHMe	trans	2.87	1.14	HF/6-31+G(d)	14
	cis	3.16	2.37		
Ac-Pro-NHMe	trans	2.58	1.37	B3LYP/6-311++G(d,p)	14
	cis	3.00	1.45		
Ac-Pro-NMe_2	trans	2.33	1.42	HF/6-31+G(d)	15
	cis	2.50	1.62		
Ac-Pro-NMe_2	trans	2.22	1.99	B3LYP/6-311++G(d,p)	15
	cis	2.73	1.94		
Ac-Hyp-NHMe	trans	3.26	2.02	HF/6-31+G(d)	this work
	cis	3.04	3.69		
Ac-Hyp-NHMe	trans	2.73	2.02	B3LYP/6-311++G(d,p)	this work
	cis	2.21	2.78		
Ac-Flp-NHMe	trans	1.74	1.63	HF/6-31+G(d)	this work
	cis	2.03	3.08		
Ac-Flp-NHMe	trans	1.01	1.76	B3LYP/6-311++G(d,p)	this work
	cis	1.38	2.41		

[a] Prolyl peptide bond. [b] Barriers calculated by Gibbs free energies ($\Delta G^{\ddagger}$) unless specified. The barriers for trans and cis peptide bonds correspond to those of the transition states ts1 and ts2 of the text as well as Tables 2 and 3, respectively. [c] Not identified as down → up or up → down puckering transitions. [d] Barriers calculated by energies ($\Delta E^{\ddagger}$).

and polyproline I (PPI), respectively, it is also observed that the prolyl ring flips from a down-puckered conformation to an up-puckered one through the transition state similar to that of Ac-Pro-NHMe for both PPII and PPI conformers.[15] At the B3LYP/6-311++G(d,p) level, the barriers to puckering transition $\Delta G^{\ddagger}_{\text{down}\rightarrow\text{up}}$ are estimated to be 2.22 and 2.73 kcal/mol for PPII and PPI conformers at room temperature, respectively, which are lower by ∼0.3 kcal/mol than those of Ac-Pro-NHMe. In Table 1, the barriers to puckering transition of various prolyl residues are summarized.

The 4(*R*)-substitution of electron-withdrawing groups such as hydroxy and fluorine at the 4-C (or C$^{\gamma}$) of the prolyl ring has resulted in substantial effects on the chemical properties of Ac-Pro-OMe.[16] With the increase of the electron-withdrawing effect, the pK_a of the prolyl nitrogen and the amide I frequency of the C═O stretching decreased. In addition, more conformers with the trans imide bond were populated with the more electronegative substituent.[16,17] The preference of the trans imide bond for Hyp and Flp residues was interpreted as the n → π^* interaction between the carbonyl oxygen preceding the prolyl residue and the carbonyl carbon of the prolyl residue by the natural bond orbital (NBO) analysis.[18] In particular, the presence of electron-withdrawing substituents has significantly affected the prolyl puckering. In crystal[19] and solution,[16,18] 4(*R*)-hydroxy-L-proline (Hyp) and 4(*R*)-fluoro-L-proline (Flp) residues strongly prefer the up puckering, whereas the unsubstituted Pro residue adopts both up and down puckerings. The preference of up puckering for the Flp residue was explained by the gauche effect in the N−C$^{\delta}$−C$^{\gamma}$−F torsion angle—the tendency to adopt the conformation with the maximum number of gauche interactions between adjacent polar bonds,[18,20] which was ascribed to the favored interactions between the C$^{\gamma}$−F antibonding orbital and the vicinal C−H bonding orbitals by NBO analyses.[18,21] The preference of trans up-puckered conformation for Hyp and Flp residues was suggested to play a role in stabilizing the collagen triple helix and its model peptides.[8,22]

We report here the results on the puckering transition of Hyp and Flp residues with trans and cis prolyl peptide bonds studied by adiabatic optimizations along the torsion angle χ^1 of the prolyl ring at the HF/6-31+G(d) level in order to figure out the effects of the 4(*R*)-substitution at the 4-C (or C$^{\gamma}$) of the prolyl ring by electron-withdrawing groups on the puckering transition. The barriers to puckering transition $\Delta G^{\ddagger}_{\text{down}\rightarrow\text{up}}$ and $\Delta G^{\ddagger}_{\text{up}\rightarrow\text{down}}$ are estimated at HF/6-31+G(d) and B3LYP/6-311++G(d,p) levels.

Computational Methods

Torsional parameters for the backbone and prolyl ring of Hyp and Flp residues are defined in Figure 1. Because the prolyl puckering was successively described by an endocyclic torsion angle χ^1 (i.e., positive and negative χ^1 for the down- and up-puckered structures, respectively),[3] the HF/6-31+G(d) energies were adiabatically optimized by varying the χ^1 value. Because of the higher barrier to rotation of the Ac−Pro peptide bond (∼13−19 kcal/mol) than the barrier to ring flip,[23] calculations were carried out only for trans and cis conformers.

All ab initio and density functional calculations were carried out using the Gaussian 98 package.[24] The values of backbone torsion angles ϕ and ψ for local minima tCd, tCu, cAu, and cAd (see the following paragraph for the definition of conformational letter codes) of Ac-Pro-NHMe optimized at the HF/6-31+G(d) level,[14,25] which were local minima for the puckering transition of Ac-Pro-NHMe,[14] were used as starting points for the empirical energy optimization of Ac-Hyp-NHMe using the ECEPP/3 force field[26] that has been used for conformational study of Pro- or Hyp-containing peptides. These minimized conformations from empirical energy calculations were used as initial structures for optimization of Ac-Hyp-NHMe at the HF/6-31+G(d) level. For each initial structure of Ac-Hyp-NHMe, three orientations, i.e., gauche+, gauche−, and trans, of the OH group were taken into account, which were defined by the torsion angle for the sequence C$^{\beta}$−C$^{\gamma}$−O$^{\delta 1}$−H. The optimization for each of local minima tCd, tCu, cAu, and cAd for Ac-Flp-NHMe at the HF/6-31+G(d) level was started from that of Ac-Pro-NHMe, in which the 4(*R*)-H atom of the Pro residue was replaced by the F atom.

Four conformations tCd, tCu, cAu, and cAd for Ac-Hyp-NHMe and Ac-Flp-NHMe optimized at the HF/6-31+G(d) level

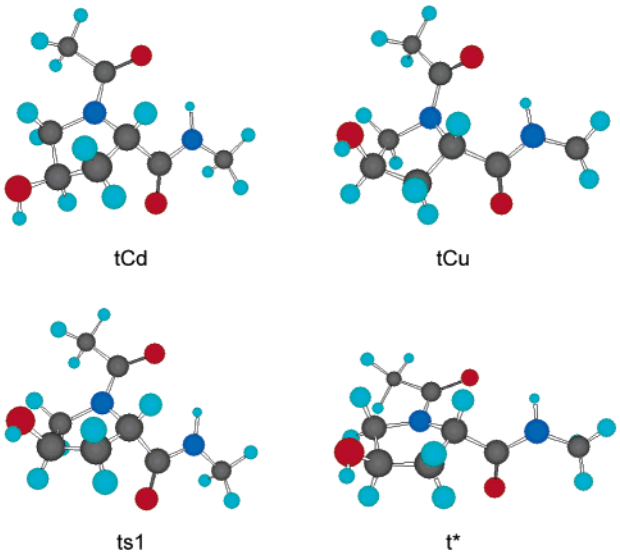

Figure 2. Structures for Ac-*trans*-Hyp-NHMe optimized at the HF/6-31+G(d) level: down-puckered structure tCd, up-puckered structure tCu, transition state structure ts1, and peak structure t*. The backbone notation C corresponds to the conformation with a C_7 intramolecular hydrogen bond between C=O of the acetyl group and H−N of the NHMe group.

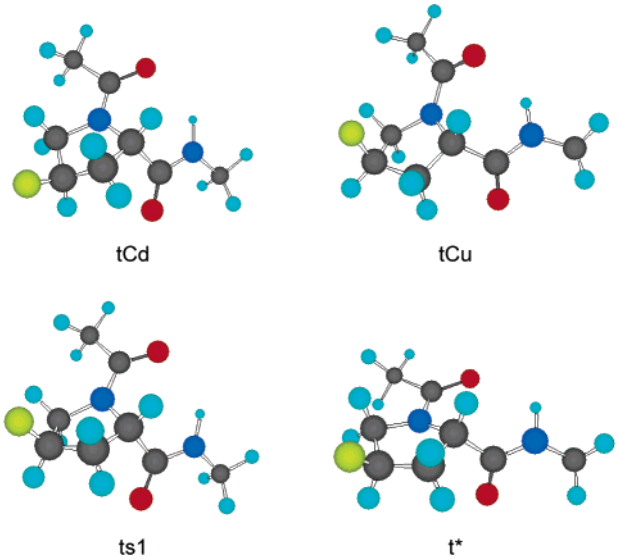

Figure 3. Structures for Ac-*trans*-Flp-NHMe optimized at the HF/6-31+G(d) level: down-puckered structure tCd, up-puckered structure tCu, transition state structure ts1, and peak structure t*. See the caption of Figure 2.

were used as starting points for adiabatic optimizations, which are shown in Figures 2 and 3, respectively. Here, each backbone conformation of Ac-Hyp-NHMe and Ac-Flp-NHMe is represented by a capital letter depending on its values of ϕ and ψ for backbone,[27] whose values are listed in Tables 2 and 3, respectively. Conformations C and A are defined by the backbone torsion angle ψ with the backbone torsion angle ϕ in the range of $-110° < \phi < -40°$: conformation C, $50° < \psi < 130°$; conformation A, $-90° < \psi < -10°$. Trans and cis conformations for the Ac−Hyp and Ac−Flp peptide bonds are defined by the orientation of the methyl carbon of acetyl group and the C^{α} of Pro residue, which are denoted by "t" and "c", respectively. Down- and up-puckered conformations are defined as those of which the C^{γ} atom and the C=O group of the prolyl residue lie on the same and opposite sides, respectively, of the plane defined by three atoms C^{δ}, N, and C^{α} (Figure 1), and are represented by "d" and "u", respectively. For example, tCd and cAu are the down-puckered conformation C with the trans prolyl peptide bond and the up-puckered conformation A with the cis prolyl peptide bond, respectively.

The structures of Ac-Hyp-NHMe and Ac-Flp-NHMe were adiabatically optimized along the torsion angle χ^1 starting from the down-puckered minimum to the up-puckered one and vice versa for each χ^1 between −40° and +40° with a step of 1° for both trans and cis conformers at the HF/6-31+G(d) level. For the conversions of trans-up to trans-down, trans-down to trans-up, cis-up to cis-down, and cis-down to cis-up, the χ^1 value spans over $-40° \le \chi^1 \le 32°$, $-16° \le \chi^1 \le 40°$, $-40° \le \chi^1 \le 30°$, and $-24° \le \chi^1 \le 40°$, respectively, for Ac-Hyp-NHMe; and $-40° \le \chi^1 \le 32°$, $-13° \le \chi^1 \le 40°$, $-40° \le \chi^1 \le 30°$, and $-23° \le \chi^1 \le 40°$, respectively, for Ac-Flp-NHMe. Local minima and transition states optimized at the HF/6-31+G(d) level were used as initial points for optimizations at the B3LYP/6-311++G(d,p) level. Vibrational frequencies were calculated for all stationary points at both levels, which were used to compute enthalpies and Gibbs free energies with scale factors of 0.89[28] and 0.98[29] at HF and B3LYP levels, respectively, at 25 °C and 1 atm. A scale factor of 0.89 at the HF/6-31+G(d) level was chosen to reproduce experimental frequencies for the amide I band of *N*-methylacetamide in Ar and N_2 matrixes.[28] A scale factor of 0.98 at the B3LYP/6-311++G(d,p) level reproduced well some experimental frequencies of proline in an Ar matrix.[29] In a recent work on proline, the B3LYP/6-311++G(d,p) level provided relative energies very close to those obtained at the extrapolated CBS CCSD(T) level and rotational constants in good agreement with experiments.[30] In addition, the B3LYP/6-311++G(d,p) level was reported to be quite effective in giving satisfactory calculated geometries for a series of organic molecules, compared to the CCSD and MP2 levels with 6-311++G(d,p) and aug-cc-pVDZ basis sets.[31]

Results and Discussion

In Tables 2 and 3, the torsion angles of the backbone and the prolyl ring for optimized local minima of Ac-Hyp-NHMe and Ac-Flp-NHMe are listed, respectively. By comparing these torsion angles and those of Ac-Pro-NHMe,[14] it can be concluded that the substitution of hydroxy and fluorine groups at the 4-C of the prolyl ring resulted in small changes in backbone and prolyl ring structures for local minima at both HF/6-31+G(d) and B3LYP/6-311++G(d,p) levels, although the substitution is known to yield substantial effects on the chemical properties of the prolyl residue.[16] For Ac-Hyp-NHMe, the largest change is found only in the torsion angle ϕ of the local minimum cAu, which is −6° at the HF/6-31+G(d) level and −5° at the B3LYP/6-311++G(d,p) level. On the other hand, the local minimum tCd has the largest change in the torsion angle ψ for Ac-Flp-NHMe, which is +7° at the HF/6-31+G(d) level and +5° at the B3LYP/6-311++G(d,p) level. In Figures 2 and 3, local minima of Ac-Hyp-NHMe and Ac-Flp-NHMe with trans imide bond optimized at the HF/6-31+G(d) level are depicted, respectively.

Relative potential energies along the torsion angle χ^1 for trans and cis conformers for Ac-Hyp-NHMe and Ac-Flp-NHMe at the HF/6-31+G(d) level are plotted in Figures 4 and 5, respectively. The optimized conformations around local minima are found to be identical for the down-to-up and up-to-down flips for both trans and cis conformers. However, different peaks are found for the down-to-up and up-to-down flips. The peaks for the up-to-down flips are identified as transition states (represented by ts1 and ts2 for trans and cis conformers,

TABLE 2: Torsion Angles and Thermodynamic Properties of Local Minima and Transition States for Ac-Hyp-NHMe Optimized at HF/6-31+G(d) and B3LYP/6-311++G(d,p) Levels[a]

conformer[b]	ω'	ϕ	ψ	ω	χ^0	χ^1	χ^2	$\chi^{3,2}$ [c]	χ^4	$\chi^{3,1}$ [d]	ΔE_e	ΔH	ΔG
						HF/6-31+G(d)							
tCd	−172.7	−86.1	77.3	−175.9	−14.0	31.8	−38.2	29.4	−9.7	−78.6	0.00	0.00	0.00
tCu	−170.4	−86.8	80.7	−174.7	−8.2	−16.1	33.2	−37.7	29.2	−62.3	1.05	1.10	1.24
ts1	−177.0	−87.0	80.7	−174.1	−29.9	17.1	0.2	−17.5	30.3	−65.7	2.66	2.12	3.26
cAu	9.9	−82.3	−19.1	−178.1	0.9	−24.0	37.4	−36.5	22.5	174.9	3.30 (0.00)	3.08 (0.00)	2.63 (0.00)
cAd	9.3	−88.1	−10.9	179.8	−11.1	29.9	−37.5	30.4	−12.0	−169.9	4.03 (0.73)	3.80 (0.72)	3.28 (0.65)
ts2	−1.2	−90.1	−1.6	178.9	−27.2	18.2	−4.0	−11.8	25.0	−174.1	6.62 (3.33)	5.89 (2.81)	6.32 (3.69)
						B3LYP/6-311++G(d,p)							
tCd	−173.0	−83.7	73.1	−176.8	−14.5	31.8	−37.7	28.4	−8.8	−78.9	0.00	0.00	0.00
tCu	−170.7	−83.9	75.5	−176.3	−8.5	−14.7	31.4	−35.9	28.3	−58.3	0.39	0.40	0.71
ts1	−176.7	−84.3	75.2	−175.5	−28.6	18.6	−3.4	−13.3	26.7	−65.3	2.01	1.48	2.73
cAu	11.5	−84.4	−16.4	−178.5	−0.6	−22.2	35.9	−35.9	23.0	171.5	3.81 (0.00)	3.64 (0.00)	3.27 (0.00)
cAd[e]	9.3	−90.6	−5.2	179.2	−14.0	31.2	−36.7	28.0	−8.7	−169.6	4.70 (0.89)	4.50 (0.86)	3.83 (0.57)
ts2	5.0	−99.8	8.8	178.5	−29.5	21.7	−7.2	−10.0	25.2	−174.4	6.12 (2.30)	5.41 (1.77)	6.05 (2.78)

[a] Angles are in degrees and energies in kilocalories per mole. For transition states, the values of ΔG correspond to barriers to puckering transition ($\Delta G^{\ddagger}_{down\rightarrow up}$ or $\Delta G^{\ddagger}_{up\rightarrow down}$), and the values of ΔE_e and ΔH are electronic and enthalpic contributions to $\Delta G^{\ddagger}$. [b] Each conformation is denoted by (1) the trans (t) or cis (c) prolyl peptide bonds, (2) the backbone conformation specified torsion angles ϕ and ψ, and (3) the down (d) or up (u) puckerings. See the text for details. [c] Equivalent to χ^3 for the Pro or Flp residues. [d] The torsion angle for the −OH group defined by the sequence $C^{\beta}-C^{\gamma}-O^{\delta 1}-H$. [e] The backbone conformation should be B according to the definition of Zimmerman et al.,[27] but it is represented as A in this work because the ψ value is just beyond the boundary $\psi = -10°$ for the backbone conformation A.

TABLE 3: Torsion Angles and Thermodynamic Properties of Local Minima and Transition States for Ac-Flp-NHMe Optimized at HF/6-31+G(d) and B3LYP/6-311++G(d,p) Levels[a]

conformer[b]	ω'	ϕ	ψ	ω	χ^0	χ^1	χ^2	χ^3	χ^4	ΔE_e	ΔH	ΔG
						HF/6-31+G(d)						
tCu	−172.0	−85.7	82.9	−174.6	−10.4	−12.7	30.0	−35.7	29.0	0.00	0.00	0.00
tCd	−174.1	−85.8	82.0	−174.9	−16.3	31.7	−36.0	25.9	−5.8	0.11	0.09	−0.11
ts1	−178.6	−85.9	84.3	−173.8	−31.2	19.8	−3.0	−15.1	29.4	1.12	0.53	1.63
cAu	6.8	−79.0	−20.1	−178.1	2.1	−23.1	35.2	−33.6	19.7	2.78 (0.00)	2.52 (0.00)	1.96 (0.00)
cAd	8.8	−88.9	−10.1	179.7	−13.0	30.3	−36.9	28.7	−9.7	3.75 (0.96)	3.56 (1.04)	3.01 (1.05)
ts2	−1.9	−89.4	−1.5	178.8	−27.0	19.4	−6.2	−9.4	23.3	5.43 (2.64)	4.65 (2.13)	5.04 (3.08)
						B3LYP/6-311++G(d,p)						
tCu	−171.7	−83.5	76.9	−176.1	−10.0	−12.1	28.8	−34.2	27.8	0.00	0.00	0.00
tCd	−174.2	−83.7	76.2	−176.1	−16.7	31.6	−35.5	25.1	−5.1	1.01	1.08	0.75
ts1	−177.7	−83.8	77.8	−175.3	−29.6	25.0	−12.7	−4.7	21.8	1.61	1.05	1.76
cAu	8.8	−81.8	−17.1	−178.6	0.3	−21.1	33.7	−33.0	20.5	4.05 (0.00)	3.84 (0.00)	3.02 (0.00)
cAd[c]	9.0	−91.9	−3.7	179.4	−16.3	31.5	−35.8	25.8	−5.8	5.22 (1.17)	5.09 (1.26)	4.05 (1.03)
ts2	4.7	−99.1	8.6	178.4	−29.0	24.0	−11.4	−5.5	21.9	5.91 (1.86)	5.19 (1.35)	5.43 (2.41)

[a] Angles are in degrees and energies in kilocalories per mole. See footnote *a* of Table 2. [b] See footnote *b* of Table 2. [c] See footnote *e* of Table 2.

respectively, in Figures 4 and 5), because each of them has one imaginary frequency after the transition state optimization, whereas the peaks for the down-to-up flips, represented by t* and c* for trans and cis conformers, respectively, are converted to the transition states ts1 and ts2, respectively, after the transition state optimization. The overall shapes of the potential energy surfaces for Ac-Hyp-NHMe and Ac-Flp-NHMe are similar to that of Ac-Pro-NHMe (see Figure 3 of ref 14), except for the changes in relative stabilities of local minima and in barriers for the puckering transition, which are discussed below.

The optimized structures for the transition state ts1 and the structure for the peak t* obtained from energy scanning at the HF/6-31+G(d) level are shown in Figures 2 and 3 for Ac-Hyp-NHMe and Ac-Flp-NHMe, respectively. Because the ts2 and c* structures are similarly puckered to the ts1 and t* ones, respectively, they are not shown separately. The peak structures t* and c* are higher in energy by 4.0 and 1.8 kcal/mol for Ac-Hyp-NHMe, and 3.4 and 1.1 kcal/mol for Ac-Flp-NHMe, than transition states ts1 and ts2, respectively, at the HF/6-31+G(d) level, whereas the corresponding values are 3.8 and 1.6 kcal/mol for Ac-Pro-NHMe, respectively.[14] The most interesting thing is that the ts1 and t* structures for Ac-Hyp-NHMe and Ac-Flp-NHMe are both envelope forms with the N atom at the top of envelope, not planar ones, as seen for Ac-Pro-NHMe.[14] In particular, two atoms C^{β} and C^{γ} are syn and anti to the C−N prolyl peptide bond in the ts1 and t* structures, respectively, which can be denoted by ${}^{N}E$ and ${}_{N}E$, respectively. Therefore, the path for the puckering transition for Ac-Hyp-NHMe and Ac-Flp-NHMe can be represented by down ↔ ${}^{N}E$ ↔ up for both trans and cis conformers, as found for Ac-Pro-NHMe.[14]

Tables 2 and 3 list torsion angles and thermodynamic properties of local minima and transition states for Ac-Hyp-NHMe and Ac-Flp-NHMe, respectively, optimized at HF/6-31+G(d) and B3LYP/6-311++G(d,p) levels. By comparing these torsion angles and those of Ac-Pro-NHMe[14] for the transition states optimized at the HF/6-31+G(d) level, it is found that the backbone torsion angles ϕ and ψ of the transition state ts2 for Ac-Hyp-NHMe and Ac-Flp-NHMe shift by −4° and +6° from those of Ac-Pro-NHMe, respectively, whereas there are small shifts in those torsion angles for the transition state ts1. The relatively larger changes in endocyclic torsion angles for Ac-Hyp-NHMe and Ac-Flp-NHMe from those of Ac-Pro-NHMe are found for the torsion angles χ^1, χ^2, and χ^3, which are calculated to be +3°, −3°, and +3° for the transition state ts1 and +5°, −5°, and +3° for the transition state ts2 of Ac-Hyp-NHMe, respectively. The corresponding changes for Ac-Flp-NHMe are computed as +5°, −6°, and +5° for the transition state ts1 and +6°, −7°, and +6° for the transition state ts2,

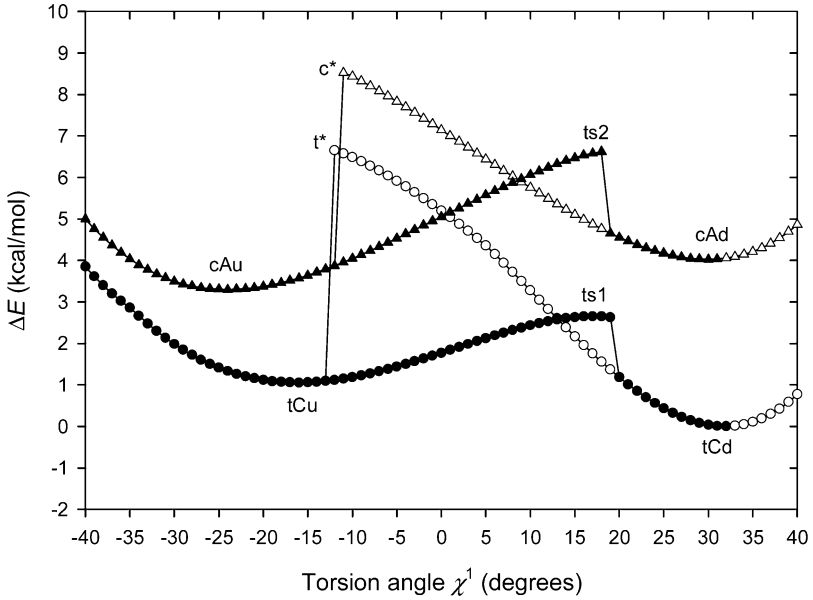

Figure 4. Relative potential energies along the torsion angle χ^1 for Ac-Hyp-NHMe. Full geometry was adiabatically optimized for each χ^1 between −40° and +40° with a step of 1° at the HF/6-31+G(d) level. The conversions for trans-up to trans-down, trans-down to trans-up, cis-up to cis-down, and cis-down to cis-up are represented by the symbols ●, ○, ▲, and △, respectively.

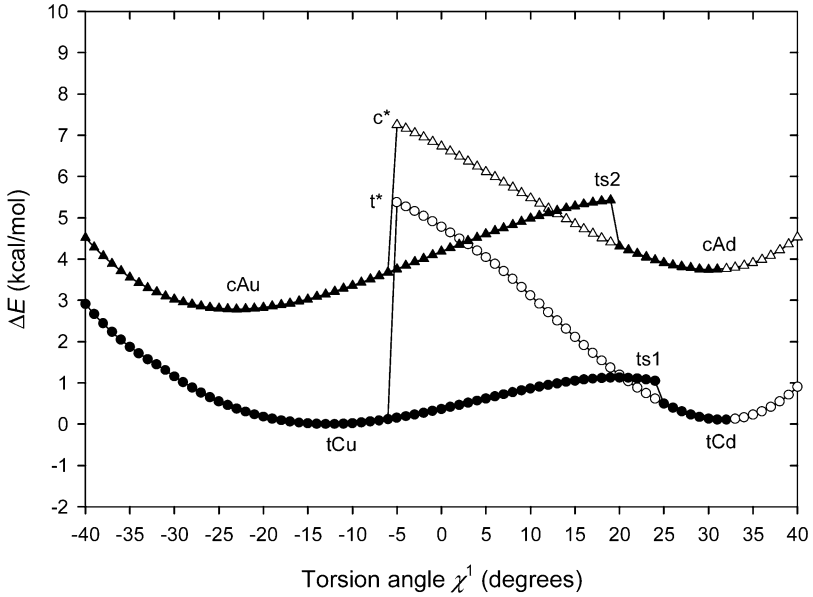

Figure 5. Relative potential energies along the torsion angle χ^1 for Ac-Flp-NHMe. See the caption of Figure 4. The conversions for trans-up to trans-down, trans-down to trans-up, cis-up to cis-down, and cis-down to cis-up are represented by the symbols ●, ○, ▲, and △, respectively.

respectively. However, the shifts in the backbone torsion angles ϕ and ψ of both transition states for Ac-Hyp-NHMe and Ac-Flp-NHMe are decreased by 3° and less at the B3LYP/6-311++G(d,p) level. On the other hand, the changes in endocyclic torsion angles χ^1, χ^2, χ^3, and χ^4 of Ac-Hyp-NHMe and Ac-Flp-NHMe from those of Ac-Pro-NHMe are more increased for the transition state ts2 of Ac-Hyp-NHMe, and for the transition states ts1 and ts2 of Ac-Flp-NHMe at the B3LYP/6-311++G(d,p) level. The calculated changes in torsion angles χ^1, χ^2, χ^3, and χ^4 are +6°, −8°, +7°, and −3° for the transition state ts1 of Ac-Hyp-NHMe, respectively; +8°, −11°, +10°, and −5° for the transition state ts1 of Ac-Flp-NHMe, respectively; and +8°, −12°, +11°, and −7° for the transition state ts2 of Ac-Flp-NHMe, respectively.

For Ac-Hyp-NHMe at the HF/6-31+G(d) level, the barriers to puckering transition from the down-puckered conformation to the up-puckered one ($\Delta G^{\ddagger}_{\text{down}\rightarrow\text{up}}$) are estimated to be 3.26 and 3.04 kcal/mol for trans and cis conformers, respectively, and the barriers to puckering transition from the up-puckered conformation to the down-puckered one ($\Delta G^{\ddagger}_{\text{up}\rightarrow\text{down}}$) are calculated as 2.02 and 3.69 kcal/mol for trans and cis conformers, respectively. For the cis conformation, the value of $\Delta G^{\ddagger}_{\text{down}\rightarrow\text{up}}$ is less than that of $\Delta G^{\ddagger}_{\text{up}\rightarrow\text{down}}$, which is ascribed to the lower conformational free energy of the up-puckered conformation than the down-puckered one. For Ac-Flp-NHMe at the HF/6-31+G(d) level, the values of $\Delta G^{\ddagger}_{\text{down}\rightarrow\text{up}}$ are estimated to be 1.74 and 2.03 kcal/mol for trans and cis conformers, respectively, and those of $\Delta G^{\ddagger}_{\text{up}\rightarrow\text{down}}$ are calculated as 1.63 and 3.08 kcal/mol for trans and cis conformers, respectively. For the trans conformers, the value of $\Delta G^{\ddagger}_{\text{down}\rightarrow\text{up}}$ is increased for Ac-Hyp-NHMe and decreased for Ac-Flp-NHMe from that of Ac-Pro-NHMe, although the down puckering is in common more stable than the up puckering. For the cis conformers, the value of $\Delta G^{\ddagger}_{\text{up}\rightarrow\text{down}}$, however, is increased for both Ac-Hyp-NHMe and Ac-Flp-NHMe from that of Ac-Pro-NHMe because the up-puckered conformation is more stable

than the down-puckered one for Ac-Hyp-NHMe and Ac-Flp-NHMe, whereas the down-puckered conformation is preferred to the up-puckered one for Ac-Pro-NHMe.[14] The preference of up puckering for the Flp residue was explained by the gauche effect in the N−C^{δ}−C^{γ}−F torsion angle—the tendency to adopt the conformation with the maximum number of gauche interactions between adjacent polar bonds,[18,20] which was ascribed to the interactions between the C^{γ}−F antibonding orbital and the vicinal C−H bonding orbitals by NBO analyses.[18,21]

For Ac-Hyp-NHMe at the B3LYP/6-311++G(d,p) level, the barriers $\Delta G^{\ddagger}_{down\rightarrow up}$ are estimated to be 2.73 and 2.21 kcal/mol for trans and cis conformers, respectively, and the barriers $\Delta G^{\ddagger}_{up\rightarrow down}$ are calculated as 2.02 and 2.78 kcal/mol for trans and cis conformers, respectively. For Ac-Flp-NHMe at the B3LYP/6-311++G(d,p) level, the values of $\Delta G^{\ddagger}_{down\rightarrow up}$ are estimated to be 1.01 and 1.38 kcal/mol for trans and cis conformers, respectively, and those of $\Delta G^{\ddagger}_{up\rightarrow down}$ are calculated as 1.76 and 2.41 kcal/mol for trans and cis conformers, respectively. Therefore, the barriers for Ac-Hyp-NHMe and Ac-Flp-NHMe at the B3LYP/6-311++G(d,p) level are lowered by −0.5 to −0.9 kcal/mol from those at the HF/6-31+G(d) level, except for the barriers $\Delta G^{\ddagger}_{up\rightarrow down}$ for trans conformers, which are almost the same at both levels. In addition, it should be noted that the changes in barriers for Ac-Hyp-NHMe and Ac-Flp-NHMe from those of Ac-Pro-NHMe have the same trend at both levels. In particular, the puckering transitions for Ac-Hyp-NHMe and Ac-Flp-NHMe are proven to be predominantly electronically driven by analyzing the electronic and enthalpic contributions to the barriers $\Delta G^{\ddagger}_{down\rightarrow up}$ and $\Delta G^{\ddagger}_{up\rightarrow down}$ calculated at HF/6-31+G(d) and B3LYP/6-311++G(d,p) levels, as seen for Ac-Pro-NHMe.[14]

Conclusions

We identified that the puckering transition of the prolyl ring for Hyp and Flp residues proceeds from the down-puckered conformation to the up-puckered one through the transition state with an envelope form having the N atom at the top of the envelope, not a planar one for both trans and cis conformers, as seen for the Pro residue. At HF/6-31+G(d) and B3LYP/6-311++G(d,p) levels, the structures of the backbone and prolyl ring for local minima of Ac-Hyp-NHMe and Ac-Flp-NHMe are quite similar to those of Ac-Pro-NHMe. However, the stability of the up-puckered conformation relative to that of the down-puckered one is increased for Ac-Hyp-NHMe with the cis imide bond and for Ac-Flp-NHMe with the trans and cis imide bonds. In particular, the 4(*R*)-substitution by hydroxy and fluorine groups has brought some structural changes in the prolyl ring of the transition states and the changes in barriers for the puckering transition.

Note Added after ASAP Publication. This article was released ASAP on August 16, 2005. In Table 3, column headings 2 through 5 have been revised. The correct version was posted on August 18, 2005.

References and Notes

(1) Richardson, J. S.; Richardson, D. C. In *Prediction of Protein Structure and the Principles of Protein Conformation*; Fasman, G. D., Ed.; Plenum: New York, 1989; p 1.
(2) Momany, F. A.; McGuire, R. F.; Burgess, A. W.; Scheraga, H. A. *J. Phys. Chem.* **1975**, *79*, 2361.
(3) Balasubramanian, R.; Lakshminarayanan, A. V.; Sabesan, M. N.; Tegoni, G.; Venkatesan, K.; Ramachandran, G. N. *Int. J. Protein Res.* **1971**, *3*, 25.
(4) DeTar, D. F.; Luthra, N. P. *J. Am. Chem. Soc.* **1977**, *99*, 1232.
(5) Madison, V. *Biopolymers* **1977**, *16*, 2671.
(6) Milner-White, E. J.; Bell, L. H.; Maccallum, P. H. *J. Mol. Biol.* **1992**, *228*, 725.
(7) Pal, D.; Chakrabarti, P. *J. Mol. Biol.* **1999**, *294*, 271.
(8) Vitagliano, L.; Berisio, R.; Mastrangelo, A.; Mazzarella, L.; Zagari, A. *Protein Sci.* **2001**, *10*, 2627.
(9) London, R. E. *J. Am. Chem. Soc.* **1978**, *100*, 2678.
(10) Sarkar, S. K.; Young, P. E.; Torchia, D. A. *J. Am. Chem. Soc.* **1986**, *108*, 6459.
(11) Mádi, Z. L.; Griesinger, C.; Ernst, R. R. *J. Am. Chem. Soc.* **1990**, *112*, 2908.
(12) Badoni, H. A.; Rodriguez, A. M.; Zamora, M. A.; Zamarbide, G. N.; Enriz, R. D.; Farkas, Ö.; Császár, P.; Torday, L. L.; Sosa, C. P.; Jàkli, I.; Perzel, A.; Papp, J. G.; Hollosi, M.; Csizmadia, I. G. *J. Mol. Struct.: THEOCHEM* **1999**, *465*, 79.
(13) Ramek, M.; Kelterer, A.-M.; Teppen, B. J.; Schäfer, L. *J. Mol. Struct.* **1995**, *352/353*, 59.
(14) Kang, Y. K. *J. Phys. Chem. B* **2004**, *108*, 5463.
(15) Kang, Y. K.; Park, H. S. *J. Mol. Struct.: THEOCHEM* **2005**, *718*, 17.
(16) Eberhardt, E. S.; Panasik, N., Jr.; Raines, R. T. *J. Am. Chem. Soc.* **1996**, *118*, 12261.
(17) Bretscher, L. E.; Jenkins, C. L.; Taylor, K. M.; DeRider, M. L.; Raines, R. T. *J. Am. Chem. Soc.* **2001**, *123*, 777.
(18) DeRider, M. L.; Wilkens, S. J.; Waddell, M. J.; Bretscher, L. E.; Weinhold, F.; Raines, R. T.; Markley, J. L. *J. Am. Chem. Soc.* **2002**, *124*, 2497.
(19) Panasik, N., Jr.; Eberhardt, E. S.; Edison, A. S.; Powell, D. R.; Raines, R. T. *Int. J. Pept. Protein Res.* **1994**, *44*, 262.
(20) Holmgren, S. K.; Bretscher, L. E.; Taylor, K. M.; Raines, R. T. *Chem. Biol.* **1999**, *6*, 63.
(21) Improta, R.; Benzi, C.; Barone, V. *J. Am. Chem. Soc.* **2001**, *123*, 12568.
(22) Jenkins, C. L.; Raines, R. T. *Nat. Prod. Rep.* **2002**, *19*, 49 and references therein.
(23) Kang, Y. K.; Choi, H. Y. *Biophys. Chem.* **2004**, *111*, 135.
(24) Frisch, M. J.; Trucks, G. W.; Schlegel, H. B.; Scuseria, G. E.; Robb, M. A.; Cheeseman, J. R.; Zakrzewski, V. G.; Montgomery, J. A., Jr.; Stratmann, R. E.; Burant, J. C.; Dapprich, S.; Millam, J. M.; Daniels, A. D.; Kudin, K. N.; Strain, M. C.; Farkas, O.; Tomasi, J.; Barone, V.; Cossi, M.; Cammi, R.; Mennucci, B.; Pomelli, C.; Adamo, C.; Clifford, S.; Ochterski, J.; Petersson, G. A.; Ayala, P. Y.; Cui, Q.; Morokuma, K.; Malick, D. K.; Rabuck, A. D.; Raghavachari, K.; Foresman, J. B.; Cioslowski, J.; Ortiz, J. V.; Baboul, A. G.; Stefanov, B. B.; Liu, G.; Liashenko, A.; Piskorz, P.; Komaromi, I.; Gomperts, R.; Martin, R. L.; Fox, D. J.; Keith, T.; Al-Laham, M. A.; Peng, C. Y.; Nanayakkara, A.; Gonzalez, C.; Challacombe, M.; Gill, P. M. W.; Johnson, B.; Chen, W.; Wong, M. W.; Andres, J. L.; Gonzalez, C.; Head-Gordon, M.; Replogle, E. S.; Pople, J. A. *Gaussian 98*, revision A.7; Gaussian, Inc.: Pittsburgh, PA, 1998.
(25) Kang, Y. K. *J. Mol. Struct.: THEOCHEM* **2004**, *675*, 37.
(26) Némethy, G.; Gibson, K. D.; Palmer, K. A.; Yoon, C. N.; Paterlini, G.; Zagari, A.; Rumsey, S.; Scheraga, H. A. *J. Phys. Chem.* **1992**, *96*, 6472.
(27) Zimmerman, S. S.; Pottle, M. S.; Némethy, G.; Scheraga, H. A. *Macromolecules* **1977**, *10*, 1.
(28) Kang, Y. K. *J. Mol. Struct.: THEOCHEM* **2001**, *546*, 183.
(29) Császár, A. G.; Perczel, A. *Prog. Biophys. Mol. Biol.* **1999**, *71*, 243.
(30) Czinki, E.; Császár, A. G. *Chem.—Eur. J.* **2003**, *9*, 1008.
(31) Wiberg, K. B. *J. Comput. Chem.* **2004**, *25*, 1342.